OPTIMAL DESIGN OF A HYDROGEN SYSTEM OF GRID-CONNECTED FLEXIBLE INDUSTRIAL MICROGRIDS

Paula Muñoz-Peña[1]* , Lorenzo Bruno[1], Aleix Señís[2], Marina Fajardo[2], Marc Cheah-Mane[1], Oriol Gomis-Bellmunt[1], Eduardo Prieto-Araujo[1]

[1]CITCEA, Universitat Politecnica de Catalunya, 647 Diagonal Avenue, Barcelona, Spain
[2]Solution Engineer, Schneider Electric. Bac de Roda 52 A, Barcelona, Spain
**E-mail: paula.munoz.pena@upc.edu*

Keywords: MICROGRID, HYDROGEN, ENERGY STORAGE, OPTIMAL DESIGN, DECARBONISATION

Abstract

Equipment redesign is needed to decarbonise energy-intensive industries, such as the glass and aluminium industries. In this context, hydrogen is proposed as fuel instead of natural gas for high-temperature heat supply. This paper presents an optimisation-based methodology to size different microgrid elements including electrolyser, compressor, hydrogen tank, and burner, alongside photovoltaic (PV) power and battery energy storage. Therefore, it aims to minimise the total costs of the system based on its operation, considering active and flexible management of generation, and costs for CO_2 emissions. Moreover, the penetration of renewables, hydrogen fraction and CO_2 emissions can be delimited. This methodology is used to analyse the role of hydrogen introduction in an industrial case study.

1 Introduction

Decarbonisation of energy-intensive industries is challenging due to their capital intensity, cost-competitiveness, and sensitivity to product quality [1]. Over 85 % of industrial heat is used by the iron and steel, chemical, and cement industries, where 95 % is based on fossil fuels nowadays [2]. In high-temperature applications, electricity can be utilised, however, industry prefers other solutions that involve minimal equipment redesign, such as hydrogen [2].

In general, the lack of optimum design can lead to power systems that are oversized or not properly planned, i.e. with higher costs. In this case, the challenge lies in matching the hydrogen production with the load, and with a combined supply of grid power and Renewable Energy Sources (RES). Energy storage can also be introduced to address the fluctuating and unpredictable nature of RES.

Power-to-Hydrogen (PtH) systems planning has been widely studied in the literature. Table 1 shows the different elements optimised in the literature. In [3], a comprehensive set of technical and economic indicators is established to analyse PtH systems, although a constant hydrogen load is supposed. Ref. [4] compares the use of hydrogen versus natural gas to supply process heat demand of a steel industry. Also, a hydrogen demand from a semiconductor industry is studied in [5] and other European sites are also analysed in [6], with the particularity that the method is rule-based. These works perform an optimal sizing of grid-connected systems, and even when renewable generation surplus is sold to the grid [3, 5], the renewable PtH system does not represent the most cost-competitive solution. Another approach is to consider the hydrogen for long-term storage in islanded systems with electric loads [7–9]. Also, both proton exchange membrane (PEM) and alkaline electrolysers can be considered, such as [8]. Ref. [9] additionally considers battery energy storage system (BESS) and electrolyser degradation cost, as well as demand response which reduces the cost of the system.

Table 1 Literature review system components

	Electric grid	PV	Wind power	BESS	Electrolyser	Compressor	H_2 tank	H_2 back-up	Fuel cell	Natural gas
[3]	✓	✓		✓	✓		✓			
[4]	✓				✓	✓	✓			✓
[5]	✓	✓			✓	✓	✓	✓		
[6]	✓	✓	✓	✓	✓		✓			
[7]		✓	✓	✓	✓		✓		✓	
[8, 9]		✓		✓	✓		✓		✓	

The analysis of the literature has revealed a gap in the PtH sizing when natural gas and renewable hydrogen are compared. Moreover, CO_2 emissions are usually not considered a decisive indicator in the optimisation of grid-connected systems, even if they are quantified for analysis or with a cost. Also, existing literature focuses on a single energy load but the combination of electrical and thermal demand is not studied.

In this context, this paper proposes an optimisation-based methodology to size the PtH system by minimising the total cost based on its operation and considering active and flexible generation management. The model considers a hydrogen

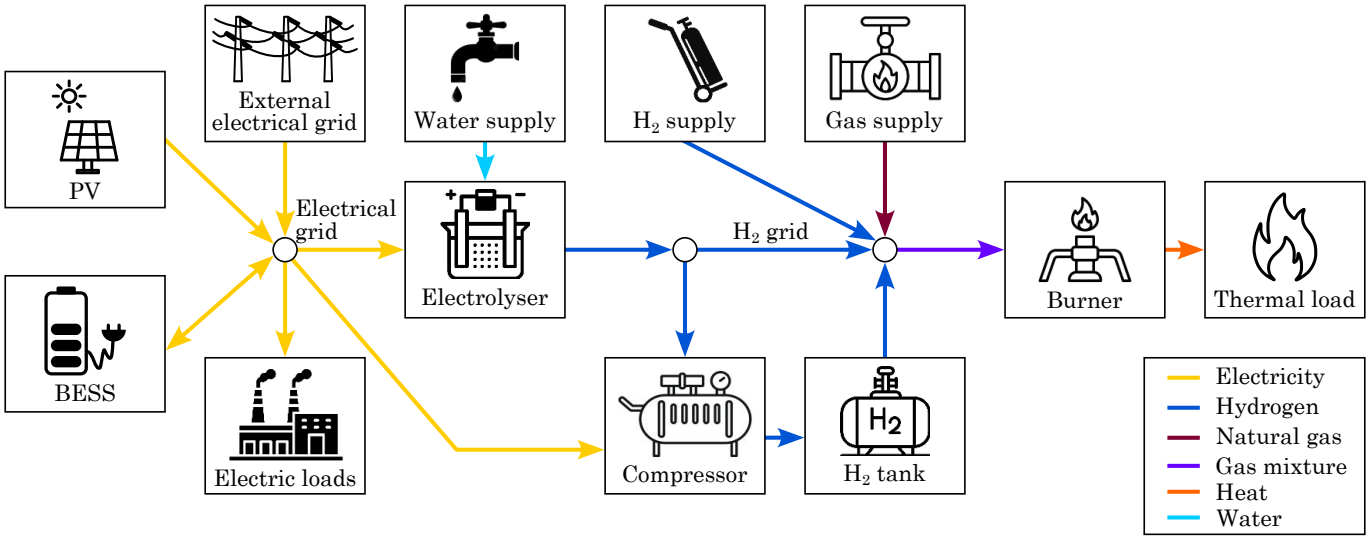

Fig. 1. System model diagram

circuit connecting a PEM electrolyser, a storage system composed of compressor and tank, and a burner. The electrolyser is powered by the electrical grid, the photovoltaic (PV) generation and BESS. Also, both electrical and thermal loads are considered, and H_2 bottle tank as backup is studied. Moreover, the thermal load is supplied through a burner that can combine hydrogen with natural gas supply. Additionally, the contracted electrical power can also be optimised. The methodology is validated in a glass industry case study which focuses on the role of hydrogen in high-temperature heat supply decarbonisation. In this paper, natural gas and renewable hydrogen compete to fuel the furnace, and CO_2 emissions are presented as the main determinant for favouring one over the other.

2 Modelling of the system components

The microgrid system to design is composed of an electrical and hydrogen grids, its layout is shown in Fig. 1. The electrical side foresees the combination of PV source, grid supply, BESS, and an electric load representing the industry consumption. The mix of electricity supplies a PEM electrolyser, where the hydrogen flow produced is split in order to feed the in parallel the furnace and the storage unit, composed of hydrogen tank and compressor. The heating system of the furnace is supposed as burner, which is used traditionally with natural gas but can also be fuelled with hydrogen from the electrolyser and storage and from a hydrogen bottled supply.

2.1 Photovoltaic system

The PV is modelled in a steady-state generator with variables related to its operation and sizing. Therefore, including active power generated ($P_{PV,t}$), defined for each hour t of the year, and the nominal power installed (to add) (P^r_{PV}). All these variables are expressed in [kW].

A single PV subsystem is supposed to have the same technical and economic characteristics of the PV module and resource forecast. Different characteristics of PV modules and forecasts can be considered by adding several PV subsystems. This approach is also applied to the other system assets.

The PV system considers a constraint related to curtailment. The power provided by each PV subsystem is positive and limited by the installed capacity and the maximum availability of the resource (forecast). Then, the active power generation limits are expressed as:

$$P_{PV,t} \leq (P^r_{PV} + P^r_{PV0}) \cdot F_{PV,t} \qquad \forall t \in [1, T] \qquad (1)$$

where $F_{PV,t}$ is the PV forecast for a specific location for each hour t in [pu], P^r_{PV0} is the existent nominal power of the PV in the system in [kW], and T is the optimisation time horizon.

2.2 Electrolyser, Compressor, Burner

The electrolyser, compressor and burner are modelled in steady-state with variables related to their operation and sizing. Operation variables are defined for each hour t of the year and expressed in [kW]. They include the electrical power input of the electrolyser and compressor ($P_{EL-in,t}$ and $P_{CP-in,t}$), hydrogen thermal power output of the electrolyser ($P_{EL-out,t}$), thermal power flow through the compressor ($P_{CP-out,t}$), thermal power input and output of the burner ($P_{B-in,t}$ and $P_{B-out,t}$). On the other hand, the sizing variables include nominal electrical power of the electrolyser and compressor (to add) (P^r_{EL} and P^r_{CP}), nominal thermal power input of the burner (to add) (P^r_B), number of electrolysers, compressors and burners (to add) (k_{EL}, $k_{CP}$and k_B). Where the nominal powers are expressed in [kW].

The electrolyser, compressor and burner constraints, expressed as element $j \in \{EL, CP, B\}$, are related to:

- Sizing in element units. The nominal power of the subsystem can be expressed as:

$$P^r_j == k_j \cdot P^r_{j1} \qquad (2)$$

where P^r_{j1} is the nominal power of a single j element unit.

- Performance. The electrolyser efficiency which relates electrical input and hydrogen output is supposed constant. Therefore, power output is expressed as:

$$P_{j-out,t} = \eta_j \cdot P_{j-in,t} \qquad \forall t \in [1,T] \tag{3}$$

where η_j is the efficiency of the j element. The compressor hydrogen power input and output of the compressor are supposed the same, and the compressor efficiency relates electrical consumption and hydrogen flow. In this case, efficiency is expressed as:

$$\eta_{CP} = \frac{LHV_{H_2}}{\tau_{CP}} \tag{4}$$

where τ_{CP} is the specific consumption of the compressor in [kWh/kg H_2], and LHV_{H_2} is the low heating value (LHV) of hydrogen in [kWh/kg H_2].

- Maximum and minimum operating power. The minimum operating power of a subsystem corresponds to the minimum operating power based on the power of a single j element unit. Maximum operating power considers the total installed capacity of the subsystem. Additionally, a binary variable ($\lambda_{j,t}$) is introduced to indicate if the subsystem is on (1) or off (0). Therefore, the power limits can be expressed as:

$$P_{j-in,t} \geq P^r_{j1} \cdot P_{j-min} \cdot \lambda_{j,t} \qquad \forall t \in [1,T] \tag{5}$$

$$P_{j-in,t} \leq (P^r_j + P^r_{j0}) \cdot P_{j-max} \cdot \lambda_{j,t} \qquad \forall t \in [1,T] \tag{6}$$

where P^r_{j0} is the existent nominal power of the j element in the system in [kW], P_{j-min} and P_{j-max} are the minimum and maximum operating power of the j element in [pu]. Instead Eq. (6), a linealised version is used with the following expressions:

$$P_{j-in,t} \leq (P^r_j + P^r_{j0}) \cdot P_{j-max} \qquad \forall t \in [1,T] \tag{7}$$

$$P_{j-in,t} \leq \lambda_{j,t} \cdot M \qquad \forall t \in [1,T] \tag{8}$$

where M is a sufficiently large value to not limit the operating power if the system is on.

2.3 Energy storage systems

Li-ion batteries as well as hydrogen tanks and bottles are considered energy storage technologies. Their steady-state modelling is analogous with variables related to their operation and sizing, therefore element $j \in \{BS, HS, HB\}$ is used in this section. Operation variables of each storage j are defined for each hour t of the year and include the charging and discharging power ($P_{j-char,t}$ and $P_{j-disch,t}$), and the energy stored ($E_{j,t}$). The sizing variables of each storage j include the maximum charging and discharging power (to add) (P^r_j), energy storage capacity (to add) (E^r_j), and number of storage units (to add) (k_j). Additionally, a variable related to the battery usage cost ($C_{use,BS}$) is considered. All power variables are expressed in [kW], energy variables in [kWh], and the cost in [€/year].

The storage constraints are related to:

- Sizing. Energy storage capacity and maximum power exchange must be proportional to those of one storage unit:

$$P^r_j = k_j \cdot P^r_{j1} \tag{9}$$

$$E^r_j = k_j \cdot E^r_{j1} \tag{10}$$

where P^r_{j1} is the maximum charging and discharging power of one unit of j element in [kW], E^r_{j1} is the energy storage capacity of one unit of j element in [kWh].

- Charging and discharging power limits of the battery are expressed as:

$$P_{BS-char,t} \leq P^r_{BS} + P^r_{BS0} \qquad \forall t \in [1,T] \tag{11}$$

$$P_{BS-disch,t} \leq P^r_{BS} + P^r_{BS0} \qquad \forall t \in [1,T] \tag{12}$$

where P^r_{BS0} is the existent maximum charging and discharging power of the battery in [kW].

- Energy stored limits, which are expressed as:

$$SOC_{j-min} \cdot (E^r_j + E^r_{j0}) \leq E_{j,t} \qquad \forall t \in [1,T] \tag{13}$$

$$E_{j,t} \leq SOC_{j-max} \cdot (E^r_j + E^r_{j0}) \qquad \forall t \in [1,T] \tag{14}$$

where SOC_{j-min} is the minimum state of charge of j element in [pu], SOC_{j-max} is the maximum state of charge of j element in [pu], E^r_{j0} is the existent energy storage capacity of j element in [kWh].

- Energy stored is expressed as:

$$E_{j,t} = \left(P_{j-char,t} \cdot \eta_{j-char} - \frac{P_{j-disch,t}}{\eta_{j-disch}}\right) \cdot \Delta t + SOC_{j,t-1} \cdot (1-\tau_j) \qquad \forall t \in [1,T] \tag{15}$$

where η_{j-char} is the charging efficiency of j element in [pu], $\eta_{j-disch}$ is the discharging efficiency of j element in [pu], Δt is the time step in $[h]$, supposed as $\Delta t = 1h$, τ_j is the energy loss ratio of the storage or self-discharge rate of j element in [pu].

- The energy stored must be the same at the beginning and the end of the year to ensure that the battery and hydrogen tank have a cycling operation. Moreover, the energy stored at the beginning of the year is unknown.

$$SOC_{BS,0} = SOC_{BS,T} \tag{16}$$

$$SOC_{HS,0} = SOC_{HS,T} \tag{17}$$

- The hydrogen supply through a bottle is supposed to be full at the start of the year and be discharged with time. Also, the hydrogen bottle can not be charged.

$$SOC_{HB,0} = SOC_{HB-max} \cdot (E_{HB} + E_{HB0}) \tag{18}$$

$$P_{HB-char,t} = 0 \qquad \forall t \in [1,T] \tag{19}$$

where E_{HB0} is the existent energy storage capacity of the hydrogen bottle in [kWh].

- To avoid the storage charge and discharge at the same time the following expression is used:

$$C_{use,BS} = c_{use,BS} \cdot \sum_{t=1}^{T} (P_{BS-char,t} + P_{BS-disch,t}) \cdot \Delta t \tag{20}$$

where $c_{use,BS}$ is the usage cost of the battery, supposed as $4 \cdot 10^{-4}$ €/kWh.

2.4 Costs modelling

The associated costs to the element $j \in \{PV, BS, EL, CP, HS, HB, B\}$ are those related to CAPEX, OPEX and replacement (if j element lifetime is lower than project lifetime).

$$C_{CAPEX,j} = c_{CAPEX,j} \cdot P^r_j \tag{21}$$

$$C_{OM,j} = c_{OM,j} \cdot (P_j^r + P_{j0}^r) \tag{22}$$

$$C_{R,j} = \sum_{y=L_j,2L_j,\ldots}^{L_{prj}} \frac{c_{R,j} \cdot (P_j^r + P_{j0}^r)}{(1+d)^y} \tag{23}$$

where $C_{CAPEX,j}$ and $C_{R,j}$ are the total capital and replacement costs of j element in [€], $C_{OM,j}$ is the total operation and maintenance cost of j element in [€/year], $c_{CAPEX,j}$ and $c_{R,j}$ are the unitary capital and replacement costs of j in [€/kW], $c_{OM,j}$ is the unitary operation and maintenance cost of j element in [€/kW/year], L_{prj} is the project lifetime in [years], L_j is the j element lifetime in [years]. The discount rate d is supposed to be 0 for simplicity. For the storage, P_j^r and P_{j0}^r in Eqs. (21) to (23) are replaced by E_j^r and E_{j0}^r.

2.5 Electrical grid connection

In systems connected to the main electrical network, the contracted power can also be optimized since its costs can depend significantly on the local energy management. In this sense, the Spanish electricity market for low, medium and high voltage is considered for electric energy purchase, although it could be straightforwardly adapted to other countries' particularities. From the Spanish regulation (BOE) specifications [10] for tariffs 2.0TD, 3.0TD, 6.1TD, 6.2TD, 6.3TD and 6.4TD, the costs associated with the energy and power terms are considered. According to the tariff, there will be a determined number of tariff periods whose contracted power can also be optimised.

Variables related to the electrical grid connection include active power supplied from the grid ($P_{egrid,t}$), defined for each hour t of the year, and contracted power (P_N), defined for each tariff period N. Both variables are expressed in [kW]. Then, the power supplied from the grid is expressed as:

$$P_{egrid,t} \leq \sum_{N=1}^{6} (P_N \cdot K_{PN,t}) \qquad \forall t \in [1,T] \tag{24}$$

where $K_{PN,t}$ is a binary that indicates the tariff period N to consider for each hour t in [pu].

The costs associated with the grid connection include the annual cost of the contracted power (C_{power}), annual cost of electric energy supplied from the grid (C_{egrid}), and annual cost of CO_2 emissions (C_{CO_2-el}), all expressed in [€/year]. Also, the annual CO_2 emissions (e_{CO_2-el}), expressed in [kg CO_2], are calculated. These costs are expressed as:

$$C_{power} = \sum_{N=1}^{6} P_N \cdot C_{PN} \tag{25}$$

$$C_{egrid} = \sum_{t=1}^{T} P_{egrid,t} \cdot \Delta t \cdot c_{egrid,t} \tag{26}$$

$$e_{CO_2-el} = \sum_{t=1}^{T} F_{CO_2-el,t} \cdot P_{egrid,t} \cdot \Delta t \tag{27}$$

$$C_{CO_2-el} = c_{CO_2} \cdot e_{CO_2-el} \tag{28}$$

where C_{PN} is the price for hiring power in the tariff period N in [€/kW/year], $c_{egrid,t}$ is the price of electric energy supply from the grid (considering both energy and access prices) for each hour t in [€/kWh]. c_{CO_2} is the price of the CO_2 emissions in [€/kg CO_2], and $F_{CO_2-el,t}$ is the CO_2 emission factor for each hour t in [kg CO_2/kWh].

2.6 Water supply

From the hydrogen production in all electrolysers, the water volume and its cost are calculated. Therefore, the annual cost of tap water (C_w) in [€] is expressed as:

$$C_w = \sum_{t=1}^{T} \frac{\sum_{EL} P_{EL-out,t} \cdot \Delta t}{LHV_{H_2}} \cdot \frac{9}{\eta_w} \cdot c_{w,t} \tag{29}$$

where η_w is the tap water treatment efficiency, and $c_{w,t}$ is the price of tap water for each hour t in [€/L].

2.7 Gas grid

The system can be connected to the natural gas grid to supply the thermal loads. Operational variables related to natural gas include thermal power supplied from the natural gas grid ($P_{gas,t}$), defined for each hour t and expressed in [kW]. The associated costs include the annual cost of the natural gas supply (C_{gas}) and the annual cost of CO_2 emissions (C_{CO_2-gas}), both expressed in [€/year]. Also, the annual CO_2 emissions (e_{CO_2-gas}), expressed in [kg CO_2], are calculated. These costs are expressed as:

$$C_{gas} = \sum_{t=1}^{T} P_{gas,t} \cdot \Delta t \cdot c_{gas,t} \tag{30}$$

$$e_{CO_2-gas} = \frac{\sum_{t=1}^{T} P_{gas,t} \cdot \Delta t}{LHV_{gas}} \cdot F_{CO_2-gas} \tag{31}$$

$$C_{CO_2-gas} = e_{CO_2-gas} \cdot c_{CO_2} \tag{32}$$

where $c_{gas,t}$ is the price of buying gas for each hour t in [€/kWh], F_{CO_2-gas} is the CO_2 emission factor in [kg CO_2/kg gas], and LHV_{gas} is the low heating value of gas in [kWh/kg gas].

3 Methodology

This section presents a methodology for designing microgrids. The objective is to size the different components, as well as define the optimum contracted power, to minimise the costs in the project's lifetime. System operation is also optimised regarding generation, storage and load management.

This methodology is based on a mixed integer linear programming (MILP) optimisation that can be expressed as Eq. (33). Fig. 2 shows a flowchart of the methodology. Objective function and constraints are detailed in the following subsections, resulting in a mixed-integer linear problem (MILP). To balance data accuracy and resolution speed, a 1-year time horizon with hourly data resolution is considered.

$$\begin{aligned} \min_{x \in \mathbb{R}^n} \quad & f(\mathbf{x}) && \text{Objective function} \\ \text{s.t.} \quad & \mathbf{g}(\mathbf{x}) \leq 0 && \text{Inequality constraints} \\ & \mathbf{h}(\mathbf{x}) = 0 && \text{Equality constraints} \end{aligned} \tag{33}$$

The methodology is applied in Python using the Pyomo package to build the optimisation model and Gurobi as a solver.

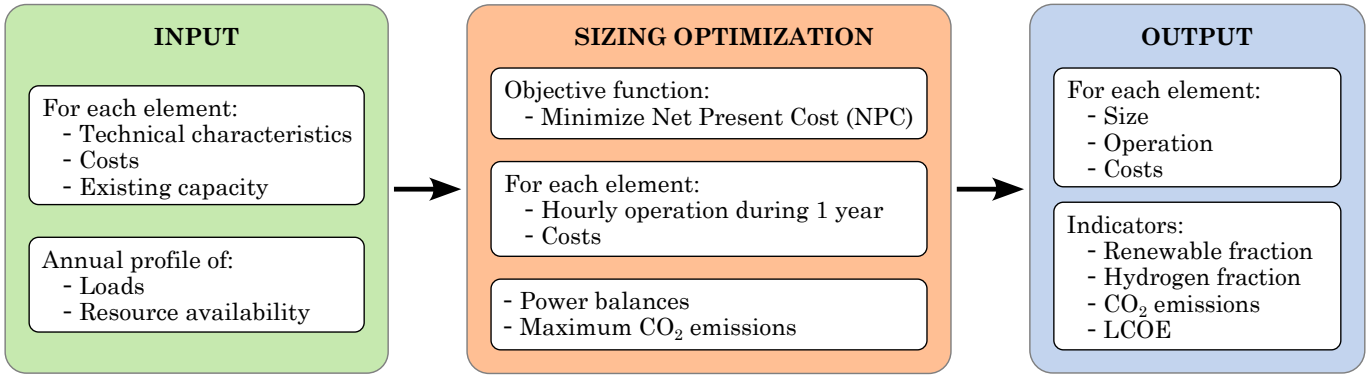

Fig. 2. Flowchart of the methodology

The algorithm considers both the elements to add and those which are already in the system. Each element is modelled separately in a subsystem and then all subsystems are connected together. Therefore, this modular approach enables to easily add new elements and features.

This methodology has been specifically developed for industrial application. Although it can also be applied to different end consumers (buildings, hospitals, etc.), as well as in energy communities, and energy hubs.

3.1 Constraints

Most of the constraints are related to the assets modelling. Therefore, all assets of the system must be considered, and, for each of them, the constraints correspond to the equations presented in Section 2.

Electric and thermal loads ($P_{eload,t}$ and $P_{thload,t}$), defined for each hour t of the year, must be supplied. Then, the power balances must be ensured, which can be expressed as:

$$P_{egrid,t} + \sum_{PV} P_{PV,t} + \sum_{BS}(P_{BS-disch,t} - P_{BS-char,t}) = \sum_{EL} P_{EL-in,t} + \sum_{CP} P_{CP-in,t} + P_{eload,t} \qquad \forall t \in [1,T] \tag{34}$$

$$\sum_{EL} P_{EL-out,t} = \sum_{CP} P_{CP-out,t} + P_{thcons,t} \qquad \forall t \in [1,T] \tag{35}$$

$$\sum_{CP} P_{CP-out,t} = \sum_{HS} P_{HS-char,t} \qquad \forall t \in [1,T] \tag{36}$$

$$P_{th-cons,t} + \sum_{HS} P_{HS-disch,t} + \sum_{HB} P_{HB-disch,t} + P_{gas,t} = P_{B-in,t} \qquad \forall t \in [1,T] \tag{37}$$

$$P_{B-out,t} = P_{thload,t} \qquad \forall t \in [1,T] \tag{38}$$

where $P_{th-cons,t}$ is the thermal power output from electrolysers that goes directly to burners.

To analyse the results, some economic indicators can be defined. In that sense, the total investment cost (C_{inv} [€]) and total annual costs (C_{annual} [€/year]) of the system are expressed as:

$$C_{inv} = \sum_{j} C_{CAPEX,j} + C_{R,j} \tag{39}$$

$$C_{annual} = \sum_{j} C_{OM,j} + C_{power} + C_{egrid} + C_{CO_2-el} + C_w + C_{gas} + C_{CO_2-gas} + C_{use,BS} \tag{40}$$

with $j \in \{PV, BS, EL, CP, HS, B\}$

Additionally, the maximum amount of CO_2 emissions (e_{CO_2-max} [kg]) can be limited as:

$$e_{CO_2-el} + e_{CO_2-gas} \leq e_{CO_2-max} \tag{41}$$

3.2 Objective function

The optimisation objective is designed to size the different assets while minimising the cost of the system through the lifetime of the project (C_{total} [€]), including the investment and the costs of each year. Therefore the objective function can be expressed as:

$$C_{total} = C_{inv} + \sum_{y=0}^{L_{prj}} \frac{C_{annual}}{(1+d)^y} \tag{42}$$

3.3 Indicators

After performing the optimisation, some indicators can be calculated. The percentage of renewable electricity supply (α_{eren} [pu]) can be considered as:

$$\sum_{t=1}^{T} \left(P_{egrid,t} \cdot F_{ren-el,t} + \sum_{PV} P_{PV,t} \right) \cdot \Delta t = \alpha_{eren} \cdot \sum_{t=1}^{T} \left(P_{egrid,t} + \sum_{PV} P_{PV,t} \right) \cdot \Delta t \tag{43}$$

where $F_{ren-el,t}$ is the renewable fraction of the electric grid for each hour t. And the hydrogen share (α_{H_2} [pu]) can be considered as:

$$\sum_{t=1}^{T} P_{gas,t} \cdot \Delta t = (1 - \alpha_{H_2}) \cdot \sum_{t=1}^{T} \sum_{B} P_{B-in,t} \cdot \Delta t \tag{44}$$

Levelised cost of thermal energy ($LCOE$ [€/kWh]) can also be used to compare different scenarios from the economic point

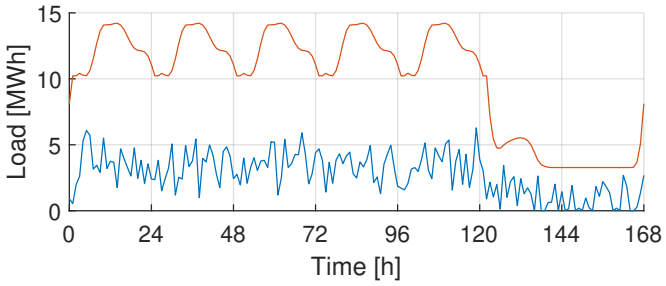

Fig. 3. Electrical (blue) and thermal (orange) load of a week

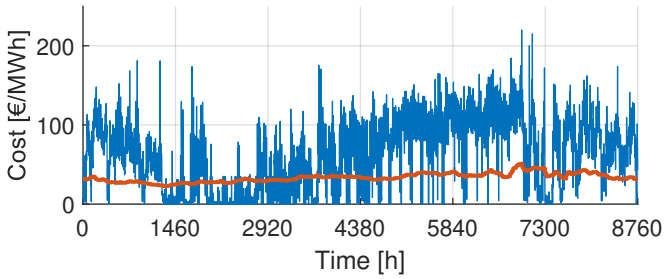

Fig. 4 Electricity (blue) and natural gas (orange) price profiles

of view. It is defined as:

$$LCOE = \frac{C_{total}}{E'} \tag{45}$$

$$E' = \sum_{y=1}^{L_{prj}} \frac{\sum_{t=1}^{T} P_{thload,t} + P_{eload,t}}{(1+d)^y} \tag{46}$$

where E' represents the actualised total load.

4 Results and discussion

4.1 Case study

The case study is based on a glass industry that consumes 85 GWh of natural gas and 25 GWh of electricity each year. Fig. 3 shows the normalised daily profiles for the application considered [11]. PV hourly forecast from Barcelona is extracted using PVGIS [12], and Li-ion batteries are considered in the electrical side of the system. A PEM electrolyser is considered for hydrogen production, which feeds the furnace and hydrogen tank with compressor. No existent power or capacity is considered for any element. The project lifetime is supposed as 20 years.

The techno-economic data of the assets are given in Tables 2 - 3 [3, 4]. The LHV of hydrogen is 120 MJ/kg. Natural gas has 48.75 MJ/kg of LHV [13] and 0.2 kg CO_2/kWh of emission factor [14]. A constant CO_2 emissions price of 70 €/t is supposed. Tap water has a constant price of 0.6 €/m^3 [15], and its treatment efficiency is 50 % [16]. Electrical grid power and energy access prices are obtained from the legislation for 2024 [17], while the hourly energy price, CO_2 emission factor and renewable fraction are extracted from ESIOS [18] for 2023/2024. Electrical grid tariff 6.3TD is supposed for this application. Hourly gas price is extracted from MIBGAS [19] for 2023/2024, with constant value along the day and an average of 33 €/MWh. Electricity and gas price profiles are shown in Fig. 4.

Table 2 Technical parameters

	Electrolyser	Compressor	Burner
Rated power	100 kW	10 kW	500 kW
Efficiency	65 %	-	98 %
Specific consumption	-	4 MJ/kg H_2	-
Minimum power	5 %	0	0
Maximum power	100 %	100 %	100 %

	Battery	H_2 tank	H_2 bottle
Rated power	100 kW	100 kW	10 kW
Storage capacity	100 kWh	100 kWh	10 kWh
SOC min	20 %	10 %	10 %
SOC max	100 %	100 %	100 %
Charging efficiency	95 %	100 %	-
Discharging efficiency	95 %	100 %	100 %
Self-discharge rate	0.007 %	0	0

Table 3 Economic parameters

	CAPEX	OPEX (annual)	Replacement cost	Lifetime (years)
PV	650 €/kW	2 %	-	20
Battery	306 €/kWh	2 %	50 %	10
Electrolyser	1188 €/kW	3 %	30 %	10
Compressor	1600 €/kW	2 %	-	20
H_2 tank	500 €/kg	2 %	-	20
Burners	63.32 €/kW$_{th}$	3 %	-	20
H_2 bottle	500 €/kg	2 %	50 %	1

4.2 Configuration analysis

Four configurations are defined based on the elements that the system considers:

- Ref.: reference configuration with only the electrical grid, gas supply and burners.
- El.: configuration adding the PV and electrolyser
- St.: configuration with BESS and hydrogen storage, including compressor and tank.
- Bot.: configuration adding the hydrogen bottled supply, as shown in Fig. 1.

The results show that the burner must be of 14.5 MW to supply the thermal load in all configurations. Renewable electricity fraction is already 47 % in Ref. configuration, and increases

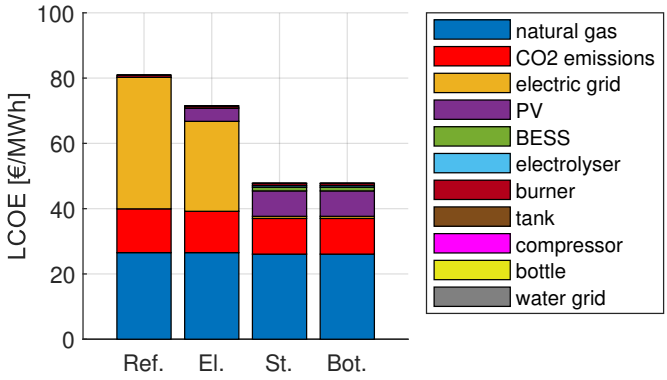

Fig. 5. Levelised cost of energy for each configuration

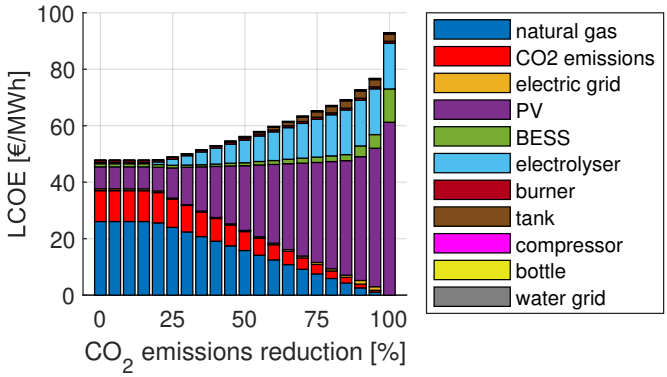

Fig. 6 Levelised cost of energy for St. configuration, as a function of the CO_2 emissions reduction factor

to 63 % in El. configuration with 9.8 MW of PV. Although, the electrolyser only appears when storage is introduced. St. configuration has a 500 kW electrolyser, resulting in a 1.7 % hydrogen share, and the renewable electricity fraction reaches 97 % with 18.8 MW of PV and 420.3 MWh BESS. In this case, the PV is prioritised over the electrical grid because the PV LCOE is around 30 €/MWh generated. And no hydrogen storage is obtained. When adding the hydrogen bottle, its costs compete with the gas. Therefore the economically optimal configuration does not have a hydrogen bottle.

The cost of each configuration is shown in Fig. 5.

4.3 CO_2 emissions analysis

The effect of limiting the CO_2 emissions is studied on St. configuration. In that sense, a reduction factor is applied to the CO_2 emissions of Ref. configuration.

From the start, St. configuration has 18 % less CO_2 emissions than Ref. configuration. With decreasing emissions, the electricity renewable fraction is kept above 97 % and the hydrogen share increases linearly. Also, the total system LCOE increases linearly from 48 €/MWh at the start, to around 69 €/MWh at 85 % emissions reduction. Regarding the cost, up to 95 % CO_2 emissions reduction can be achieved if the industry is willing to spend as much as the Ref. configuration on the

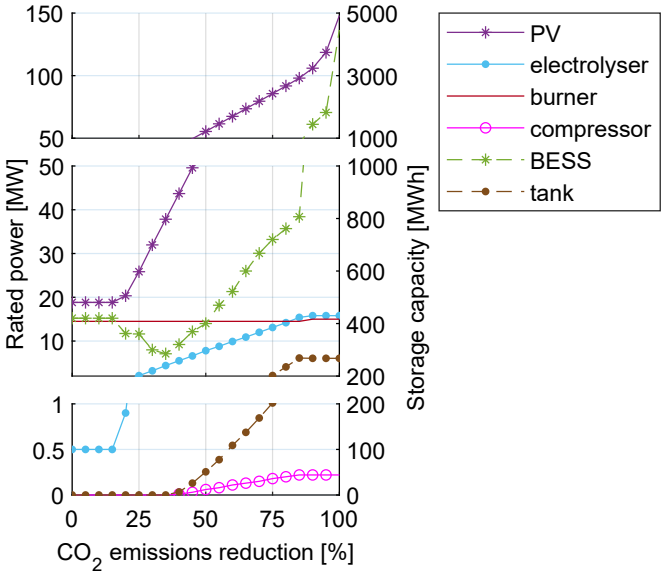

Fig. 7 Rated power and storage capacity of each element for St. configuration, as a function of the CO_2 emissions reduction factor

energy cost. Fig. 6 shows that the cost predominant elements are the PV, electrolyser and natural gas.

The installed capacity of the different elements is shown in Fig 7, where PV and electrolyser increase linearly between 20 % and 85 % CO_2 emissions reduction factor. Hydrogen storage is introduced when the CO_2 emissions are imposed to be less than 40 % of the Ref. configuration. Hydrogen tank and compressor increase linearly between 40 % and 85 % CO_2 emissions reduction. A significant difference between rated power and storage capacity is observed in hydrogen storage, as the compressor can reach up to 200 kW while the hydrogen tank is in the order of tens to hundreds of MW. On the other hand, the battery storage capacity decreases between 20 % and 35 %, as increasing the PV and electrolyser has lower costs than increasing the battery to reach the same amount of CO_2 emissions. But from 40 % to 85 % of emissions reduction, the battery storage capacity increases linearly together with the rest of the elements.

Finally, the size of hydrogen system elements stabilises when trying to reach a low amount of CO_2 emissions. This means that, from 85 % emissions reduction, the thermal load could be supplied only with hydrogen, but gas supply is preferred during the operation due to its low cost compared with electricity. With low CO_2 emissions, also the electricity must come mainly from renewable sources, and the unpredictable and variable nature of solar energy leads to oversizing of PV and battery storage. Therefore, PV and BESS increase exponentially from 85 % emissions reduction.

5 Conclusion

This paper analysed the role of hydrogen to decarbonise energy-intensive industries. A methodology was presented to size the PV, battery energy storage, electrolyser, hydrogen

storage composed of compressor and tank, and burner. The methodology is based on an optimisation problem that includes system operation to minimise the total costs. Technical and economic indicators are also provided.

This methodology was validated in a case study based on a glass industry. The effect of adding and sizing the different elements concludes that a hydrogen system is not economically optimum with the current gas prices, if other aspects are not considered. However, the electrolyser rated power and hydrogen storage capacity increase together with the PV and BESS when CO_2 emissions are progressively reduced. Therefore, as a general conclusion, the results showed that the hydrogen system is feasible if CO_2 emissions are limited. Similar results could be obtained if CO_2 costs increase instead of limiting the emissions. The proposed planning methodology employs a deterministic approach. Considering the long time horizon involved, future works can include uncertainties and a sensitivity analysis of costs.

At the end, natural gas supply is the current solution for energy-intensive industries. Nevertheless, renewable electrification and hydrogen are necessary to achieve a decarbonised energy system, additional incentives or cost reductions should happen to enable a fully decarbonised system.

6 Acknowledgements

This work is funded by the European Union's Horizon Europe research and innovation programme in the framework of the project "H2GLASS" with grant agreement number 101092153. This work is also developed in collaboration with Schneider Electric.

The work of Marc Cheah-Mane and Eduardo Prieto-Araujo was supported by the Serra Hunter Programme. The work of Oriol Gomis-Bellmunt was supported by the ICREA Academia program. The work of Paula Muñoz-Peña was supported by the predoctoral program AGAUR-FI grant (grant number 2023 FI-1 00687) Joan Oró from Secretaria d'Universitats i Recerca del Departament de Recerca i Universitats de la Generalitat de Catalunya and the European Social Fund Plus.

7 References

[1] M. Zier, P. Stenzel, L. Kotzur, and D. Stolten, "A review of decarbonization options for the glass industry," *Energy Conversion and Management: X*, vol. 10, p. 100083, 2021.

[2] IRENA, "Green hydrogen for industry: A guide to policy making," International Renewable Energy Agency, Abu Dhabi, Tech. Rep., 2022.

[3] P. Marocco, M. Gandiglio, and M. Santarelli, "Optimal design of pv-based grid-connected hydrogen production systems," *Journal of Cleaner Production*, vol. 434, p. 140007, 2024.

[4] P. Marocco, M. Gandiglio, D. Audisio, and M. Santarelli, "Assessment of the role of hydrogen to produce high-temperature heat in the steel industry," *Journal of Cleaner Production*, vol. 388, p. 135969, 2023.

[5] M. G. Davide Trapani, Paolo Marocco and M. Santarelli, "Optimal design of renewable power-to-hydrogen system for the decarbonization of a semiconductor industry." Las Palmas De Gran Canaria, Spain: ECOS 2023.

[6] M. Stolte, F. D. Minuto, and A. Lanzini, "Optimizing green hydrogen production from wind and solar for hard-to-abate industrial sectors across multiple sites in europe," *International Journal of Hydrogen Energy*, vol. 79, pp. 1201–1214, 2024.

[7] P. Marocco, D. Ferrero, A. Lanzini, and M. Santarelli, "The role of hydrogen in the optimal design of off-grid hybrid renewable energy systems," *Journal of Energy Storage*, vol. 46, p. 103893, 2022.

[8] ——, "Optimal design of stand-alone solutions based on RES + hydrogen storage feeding off-grid communities," *Energy Conversion and Management*, vol. 238, p. 114147, 2021.

[9] P. Marocco, D. Ferrero, E. Martelli, M. Santarelli, and A. Lanzini, "An milp approach for the optimal design of renewable battery-hydrogen energy systems for off-grid insular communities," *Energy Conversion and Management*, vol. 245, p. 114564, 2021.

[10] BOE, "Circular 3/2020, de 15 de enero, de la comisión nacional de los mercados y la competencia, por la que se establece la metodología para el cálculo de los peajes de transporte y distribución de electricidad," [Online].

[11] A. Sandhaas, "Generation of industrial electricity and heat demand profiles for energy system analysis," 2022. [Online]. Available: https://api.semanticscholar.org/CorpusID:260512020

[12] European Comission, "Photovoltaic Geographical Information System." [Online]. Available: https://re.jrc.ec.europa.eu/pvg_tools/en/

[13] Ministerio para la transición ecológica y el reto demográfico, "Anexo 7. Factores de emisión de CO_2 y PCI de los combustibles," [Online].

[14] Our World in Data, "Carbon dioxide emissions factors." [Online]. Available: https://ourworldindata.org/grapher/carbon-dioxide-emissions-factor

[15] Aigües de Barcelona, "La factura del agua para suministros comerciales/industriales," [Online].

[16] L. Setti and S. Sandri, "Studio sulla sostenibilità economica dellafiliera di produzione di idrogeno verde per una hydrogen backbone italiana," International Renewable Energy Agency, Abu Dhabi, Tech. Rep., 2022.

[17] BOE, "Resolución de 21 de diciembre de 2023, de la Comisión Nacional de los Mercados y la Competencia, por la que se establecen los valores de los peajes de acceso a las redes de transporte y distribución de electricidad de aplicación a partir del 1 de enero de 2024," [Online].

[18] ESIOS, "Precio mercado SPOT Diario." [Online]. Available: https://www.esios.ree.es

[19] MIBGAS, "Price and volume Index per gas day." [Online]. Available: https://www.mibgas.es/en/market-results/gas-daily-price-index-and-volumes